12th International Symposium on Turbulence and Shear Flow Phenomena (TSFP12)
Osaka, Japan (Online), July 19-22, 2022

EXPLICIT ALGEBRAIC REYNOLDS STRESS MODELLING IN SCALE-RESOLVED SIMULATIONS OF TURBULENCE

Matteo Montecchia
Department of Engineering Mechanics
KTH, Royal Institute of Technology
Osquars Backe 18, SE-10044 Stockholm, Sweden
matteomo@mech.kth.se

Stefan Wallin
Department of Engineering Mechanics
KTH, Royal Institute of Technology
Osquars Backe 18, SE-10044 Stockholm, Sweden
stefanw@mech.kth.se

ABSTRACT

New hybrid RANS/LES methods are proposed where explicit algebraic Reynolds stress modelling is introduced both in the RANS and LES regions. Both in the form of an IDDES method allowing for wall-modelled LES simulations and in the form of an DDES methods where attached boundary layers are shielded within RANS. The methods are extensions of the SST-(I)DDES metods by Gritskevich, et al., Flow, turbulence and combustion 88 (3), 431?449, 2012. In channel flow the log region is well predicted for different Reynolds numbers similar as with the baseline SST-IDDES, but the EARSM-IDDES give a more rapid transition to turbulence closer to the wall. The model gives reasonable results on very coarse meshes, basically similar with the baseline SST-IDDES, for periodic hill flow at $Re = 10.000$ and 37.000 Also for the 3D Stanford diffuser, the EARSM-IDDES gives good results, here superior to the SST-IDDES, which has problems in fully resolving the turbulence in the inlet channel. The model in DDES mode is tested on the developing shear layer. The so-called grey area problem is substantially mitigated compared with the SST-DDES resulting in a more physically correct and fully developed resolved turbulence.

INTRODUCTION

Standard eddy-viscosity models (EVMs) are widely used for RANS models as well as for modelling the unresolved scales in scale-resolved simulations (e.g. LES) due to their simplicity and stability. These models have, however, a number of well known problems associated with the linear relation between the velocity strain rate and the turbulence stresses resulting in inadequate representation of the stress anisotropy and turbulence production insensitive of local rotation, e.g. swirl, and mean-flow curvature. Physical realisability is easily violated due to the fact that the modelled Reynolds stress components are not restricted by the turbulence kinetic energy.

Explicit algebraic Reynolds stress models (EARSM) formally derived from applying the weak-equilibrium assumption on the full Reynolds stress transport models are now established for RANS modelling, e.g. Wallin & Johansson (2000), where many of the problems associated with eddy-viscosity models are mitigated without major increase in computational effort or degeneration of numerical stability.

Application of EARSM for scale-resolved simulations cannot be strictly based on the weak-equilibrium assumption, which is not well established on the resolved time-dependent scales. Equilibrium is only reached in an averaged sense, which to some degree can motivate the use of EARSM for subgrid modelling, though. Nevertheless, SGS models for LES containing non-linear terms inspired by EARSM have been shown to give improvements where the SGS anisotropies are of importance, e.g. in the near-wall regions of wall-resolved LES, see Marstorp *et al.* (2009), Montecchia *et al.* (2017) and Montecchia *et al.* (2018).

Scale-resolved simulations with unified modelling of the unresolved turbulence with variable resolution ranging from RANS to LES, or even DNS if sufficiently resolved. Such "hybrid RANS/LES" modelling is an active research field since the work of Spalart (2009). One of the fundamental problems with such modelling is the transition regions with rapid changes of resolution. Formulation of the filter commutation terms and corresponding energy-conserving modelling is proposed by Girimaji & Wallin (2013), Kamble *et al.* (2022).

Introduction of EARSM for hybrid RANS/LES models in the RANS region can be motivated by the need for better representation of attached boundary layers and separation onset from smooth surfaces, which to a large extent is driven by the RANS modelling, see e.g. Jaffrézic & Breuer (2008). For consistency between RANS and LES modelling and for utilising possible benefits in the LES region, we will introduce a unified EARSM in both RANS and LES regions as well as in the transition in between. This will be further elaborated in the paper for flows in simple and more complex geometries. The extension of the modelling accounting for the commutation terms in the transition regions will be left for later studies.

MODEL FORMULATION

Explicit Algebraic Reynolds stress model (EARSM) formulation for the Reynolds stress tensor can be written as:

$$\overline{u_i'u_j'} = \frac{2}{3}k\delta_{ij} + \beta_1 k\tau^* S_{ij} + \beta_4 k\tau^{*2}(S_{ik}\Omega_{kj} - \Omega_{ik}S_{kj}) + \ hot's. \tag{1}$$

where S_{ij} and Ω_{ij} are the dimensional resolved symmetric strain and antisymmetric rotations rate tensors, respectively, such as $\nabla U = S + \Omega$ and τ^* the modelled turbulence time scale. The formulation and derivation follow the work by Wallin & Johansson (2000), but here without the normalisation.

The β's depend on invariants of S_{ij} and Ω_{ij} resulting from the formal solution of the differential Reynolds stress model equations in the weak-equilibrium limit where variation of Reynolds stress anisotropy is neglected. The second term on the right-hand-side of (1) is an eddy-viscosity term while the third non-linear term aims to improve the modelling of stress anisotropy. High-order terms account for 3-D effects.

The second, eddy-viscosity, term will have an effective viscosity

$$\nu_T^{\text{eff}} = -\frac{1}{2}\beta_1 k\tau^* \tag{2}$$

with a non-constant effective $C_\mu = -\beta_1/2$, where β_1 is given from the EARSM solution of Wallin & Johansson (2000).

The adaptation of expression (1) as a sub-grid scale (SGS) model for scale-resolved simulations is not strictly motivated from the weak-equilibrium. Hence, it can be considered as a truncation of the full EARSM retaining terms up to the third term in (1) and does not consider higher order terms. The second, eddy-viscosity, term is dissipative while the third term is basically redistributive and non-dissipative contributing to the anisotropy.

A further step in the modelling explored in this study is the adoption of the EARSM relation (1) for hybrid RANS-LES computations. For this purpose we will extend the existing SST $k-\omega$ IDDES and DDES methodologies of Gritskevich *et al.* (2012), by replacing the eddy-viscosity relation with the EARSM formulation. In the RANS region the full 3D formulation including high order terms will be used, while in the LES region only terms up to second order are kept.

The blending between LES and RANS stress is made by the use of the $\widetilde{f}_d$ and f_d blending functions, respectively, as defined in Gritskevich *et al.* (2012) without further adaption or tuning. The blending functions are functions of an eddy viscosity and here the SST viscosity is used, $\widetilde{f}_d(\nu_T^{\text{SST}})$ and $f_d(\nu_T^{\text{SST}})$, for closest consistency with the original definition.

Consistently with the original model, the DDES mode is used for detached eddy simulations where the whole boundary layer is shielded to be purely within the RANS zone. The IDDES mode is an extension where the RANS-LES interface will be located well inside of the boundary layer if the grid resolution is fine enough to allow wall-modelled LES.

When EARSM is adopted in RANS modelling, the estimation of kinetic energy and turbulence time scale is performed by employing model transport equations for the turbulent kinetic energy k and a length-scale determining quantity, e.g. ε or ω, the latter applied in this work. For consistency with the SST $k-\omega$ (I)DDES modelling of Gritskevich *et al.* (2012), we are using the model transport equations for k and ω for determining the resolved scales in both RANS and LES modes. This is contrary of our earlier work on EARSM for WRLES, where the subgrid turbulence kinetic energy was employed from a dynamic procedure, in the same spirit of Germano *et al.* (1991) (Marstorp *et al.* (2009), Montecchia (2019)). A possible further development could be to adopt the dynamic procedure also in the LES regions of the (I)DDES.

The $k-\omega$ model equations are adopted as defined in Gritskevich *et al.* (2012), with the important difference that the turbulence production is not modelled through the eddy-viscosity assumption, but defined without further modelling through the EARSM as

$$\mathscr{P}_k = -\overline{u_i'u_j'}\frac{\partial U_i}{\partial x_j}. \tag{3}$$

The coefficients are all following Wallin & Johansson (2000), except the recalibration of A_1 for a precise consistency with the Menter BSL/SST model. Then, $c_{1,\text{RANS}} = 1.8$ and $A_1 = 1.245$. The Rotta constant c_1 in LES requires further considerations involving local flow and Re dependencies, see Marstorp *et al.* (2009). Moreover, we are utilising that the SGS k is estimated from the transport equation, resulting in

$$c_{1,\text{LES}} = c_1'\sqrt{c_3'}\frac{k^{1.25}}{(2C_s\Delta S)^{2.5}}. \tag{4}$$

with $c_1' = 4.2$, $c_3' = 2.4$, $C_s = 0.1$ and $A_1 = 1.65$.

The time scale $\tau = k/\varepsilon$ is further approximated by Marstorp *et al.* (2009). By replacing the dynamic procedure with the transport equation for k we deduce

$$\tau_{\text{LES}} = c_3' 1.5 C^{1.5}\frac{\sqrt{k}}{2C_s\Delta S^2}, \tag{5}$$

where $C = 0.5$ is the Kolmogorov constant.

All coefficients and model details that differ between RANS and LES are blended by $\widetilde{f}_d$ and f_d blending functions before the EARSM solution is obtained for the mixed anisotropies. Also, N and $\beta_{3,6,9}$ are blended.

RESULTS

The Explicit Algebraic subgrid-stress model (EAM) was previously extensively validated and tested for wall-resolved large-eddy simulations (WRLES) of turbulent channel flow at a range of Reynolds numbers up to $Re_\tau = 5200$. Both a specific solver with spectral accuracy and the general-purpose OpenFOAM solver have been used. The resolution requirement for wall-resolved LES scales with the near-wall viscous scales and is almost as high as for DNS. We found that EARSM as a SGS model could relax the resolution requirements compared with the dynamic Smagorinsky model. One example of mean velocity profiles are shown in figures 1 at different Reynolds numbers. As throughly described in (Montecchia *et al.* (2017), Montecchia *et al.* (2019)) the EAM has also improved the estimation of Reynolds stresses, in particular of the diagonal components. These improvements have been consistently observed for all Reynolds numbers and for solvers with high numerical accuracy as well as standard general purpose CFD solvers.

IDDES RESULTS

The development of the EARSM-IDDES has been implemented into OpenFOAM and was validated and tested for turbulent channel flows at $Re_\tau = 934$ and 5200. The number of grid points in the stream- and spanwise directions are the same 60×60 for both Re resulting in that the grid resolutions in wall units are $(\Delta x^+, \Delta z^+) = (98, 49)$ and $(544, 272)$, respectively for the two Reynolds numbers, resulting in less than a half million grid points. The wall-normal resolution is set such that $y^+ \sim 1$ at the first cell.

Mean velocity profiles, shown in figure 2 are reasonably computed by EARSM-IDDES and the $k-\omega$ SST IDDES for both Reynolds numbers. The log-layer mismatch is quite limited for both models. However, the transition from the near-wall RANS to LES is located closer to the wall and is more rapid for the EARSM-IDDES, resulting in a considerably larger amount of resolved turbulence near the wall seen in the figure. Although, the more rapid transition for the EARSM-IDDES induces slightly less accurate log profiles but might be of importance in mitigating the so called grey-area problems in more complex cases.

The EARSM-IDDES was further tested by the computation of the periodic hill flow Mellen *et al.* (2000) at bulk Reynolds numbers of $Re_b = 10595$ and $Re_b = 37000$. The wall-normal resolution is $y^+ \sim 1$ at the first cell, while the number of grid points along the streamwise and spanwise directions are about 70×46. The grids for both cases are, hence, very coarse with less than half million grid points to be able to observe influence of modelling. The flow as well as the Reynolds number dependency is reasonably captured by the new model on these coarse meshes, see figure 3. SST-IDDES performs slightly better in the separated region and capturing the peak at the hill crest, while EARSM-IDDES captures the reattachment point slightly better.

The 3-D diffuser case by Cherry *et al.* (2008), also simulated by DNS by Ohlsson *et al.* (2010) at the lower Re, is a more difficult case to compute where the corner vortices in the inflow duct play a major role in the development of the asymmetrical separation. Two different Reynolds numbers were computed, at $Re_h = 10000$ and $Re_h = 30000$. Two different grids are used, a "coarse" one of 1.4 and a "fine" one of 2.8 million grid points. Pressure coefficient as a function of the streamwise direction at $Re_h = 10000$ and $Re_h = 30000$ is shown in figure 5. The coarse resolution could not well capture the flow and will not be further considered. For the fine resolution, both models provide a similar prediction of the pressure coefficient at the lower Reynolds number. At the higher Reynolds number, EARSM-IDDES gives a significant improved C_p compared to SST-IDDES. No DNS is yet

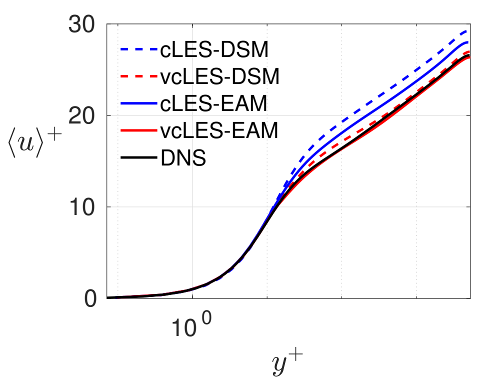

Figure 1. Inner-scaled mean velocity profile computed from WRLES at $Re_\tau \approx 5200$, with two different resolutions. vcLES: $(\Delta x^+, \Delta z^+) = (255, 102)$, cLES: $(\Delta x^+, \Delta z^+) = (159, 64)$. EAM compared with dynamic Smagorinsky as SGS model.

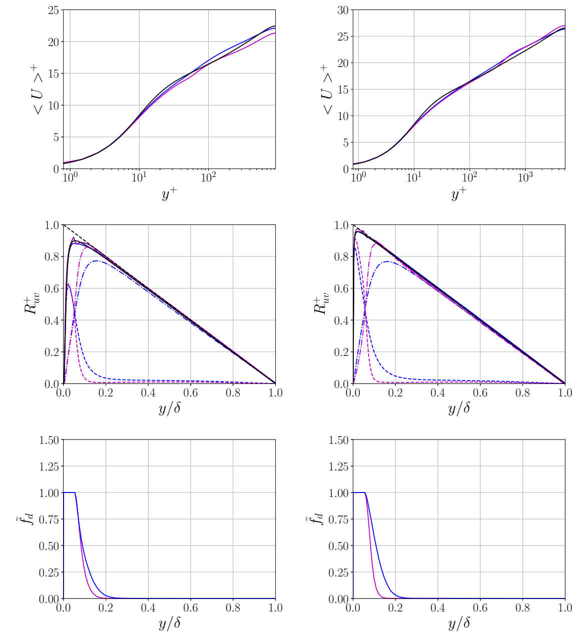

Figure 2. Channel flow simulation using IDDES showing inner-scaled mean velocity profile, Reynolds shear stress and the blending function $\widetilde{f}_d$ for $Re_\tau \approx 950$ (left) and $Re_\tau \approx 5200$ (right). —— : $k-\omega$ SST-IDDES, —— : EARSM-IDDES, —— : DNS. The turbulence shear stress is divided into modelled $(---)$ and resolved $(-\cdot-)$ contributions.

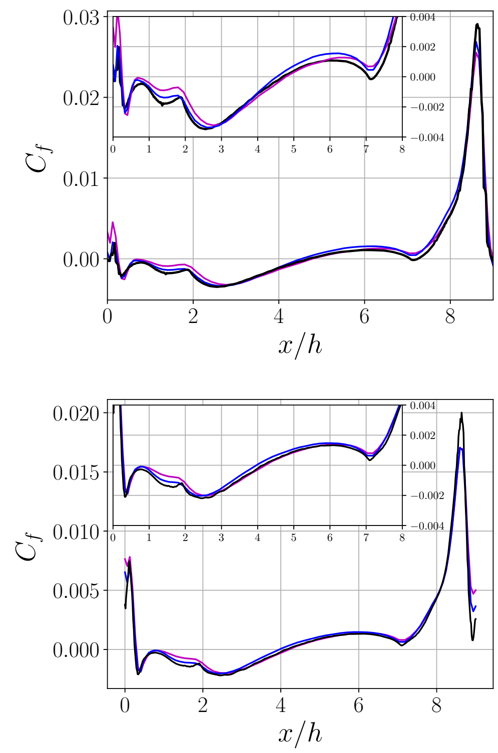

Figure 3. Periodic hill simulation using IDDES showing lower wall skin friction for $Re_b = 10595$ (top) and $Re_b = 37000$ (bottom). —— : $k-\omega$ SST-IDDES, —— : EARSM-IDDES, —— : DNS.

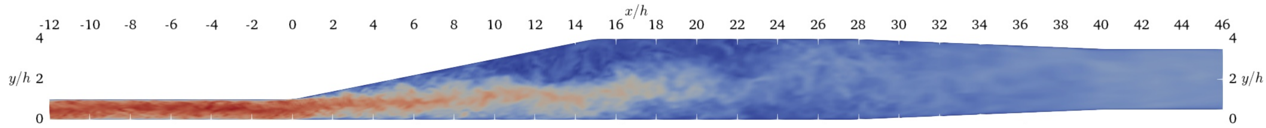

Figure 4. Colorplot of the streamwise velocity along the mid-span plane at $Re_h = 10000$.

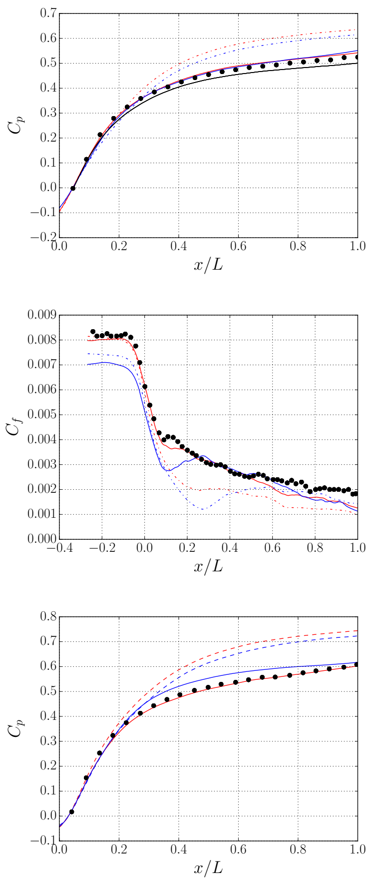

Figure 5. 3D diffuser simulations. Pressure and friction coefficients, C_p and C_f, along the streamwise direction at $z/B = 0.5$ for $Re_h = 10000$ (top, middle) and 30000 (bottom) computed using EARSM-IDDES (red) and SST-IDDES (blue) for fine (solid lines) and coarse (dashed-dotted lines) meshes. Compared with reference DNS (black lines) and experimental (black symbols) data.

available, so C_f cannot be compared for the high Re case. At $Re_h = 10000$ the friction coefficient is better predicted by using EARSM-IDDES, the inlet duct is affected by the largest improvements, where SST-IDDES fails to resolve the fully developed turbulence at the inlet channel. The improvements related to the inlet channel for EARSM-IDDES might be related to the more near-wall transition from RANS to LES seen in the channel flow above.

DDES RESULTS

Also the development of the EARSM-DDES was implemented into OpenFOAM. Here, the boundary layers are shielded and completely in RANS mode. Validation of DDES models are difficult since it will involve cases with both thin attached boundary layers and free turbulence, which are cases more complex than typical generic benchmark cases.

We will here use a developing free shear layer as a test case. This case was previously described in the EU project Go4Hybrid Mockett *et al.* (2018) and is of particular interest for hybrid RANS-LES methods due to that fully developed thick boundary layers are advected into a free shear layer with a transition from RANS to LES. Standard DES methods have shown severe suppression and delay of the developing of resolved turbulence in the shear layer, the so-called grey-area problem.

The analysis of the turbulent structures, depicted in figure 6, shows that EARSM-DDES, differently from $k-\omega$ SST-DDES, has a much faster RANS to LES transition, and a much shorter extent of the grey area. The blending function f_d shows similar transition from RANS to LES for both models shown as iso-lines of f_d in figure 7 very near the flat-plate trailing edge. Instead, SST-DDES shows a locally higher SGS shear stress in this region while EARSM-DDES predicts lower SGS shear stress. The SGS shear stress is closely connected to the SGS dissipation. This plot clearly illustrates that the grey area reduction by EARSM is mostly due to the refined and more physical Reynolds stress modelling and not due to differences in the blending function. It is known that the EARSM in RANS mode is better responding to the rapid shear avoiding the severe unphysical over-prediction of modelled turbulence observed from eddy-viscosity models. Our hypothesis is that EARSM for the same reason will preserve a more physical SGS stress in the transition region compared with SST-DDES. On the other hand, the SST k-ω model does have an eddy-viscosity limiter which is supposed to mitigate this particular problem, and it is not clear why this is not reflected in the results shown here.

The resulting velocity profiles are shown in figure 8 at two different x positions. The first position is in the later initial transient while the second position is where the shear layer can be considered to be fully developed. At both positions the EARSM-DDES is superior to the SST-DDES, which is a reflection of the very damped and delayed transition seen in the SST-DDES results. The corresponding Reynolds stresses (or $\overline{u'_i u'_j}$) are shown in figure 9 for the later fully developed position. EARSM-DDES here shows a good representation of the different components.

CONCLUDING REMARKS

The introduction of EARSM for hybrid RANS/LES simulations is primarily expected to give improvements for attached boundary layers and initial separation from smooth surfaces when 3D effects and curvature/rotation is present. Incorporating EARSM in both RANS and LES regions is mainly motivated for consistency reasons, with less expected incompatibilities in the interface regions. Also our previous studies on WRLES indicate that some improvements could be expected also in the pure LES regions.

It was found that the interface regions were particularly influenced by the novel modelling, which was somewhat unexpected. That can partly be explained by that the blending function reacts differently when used for EARSM even though the formulation is kept as close as possible with the baseline

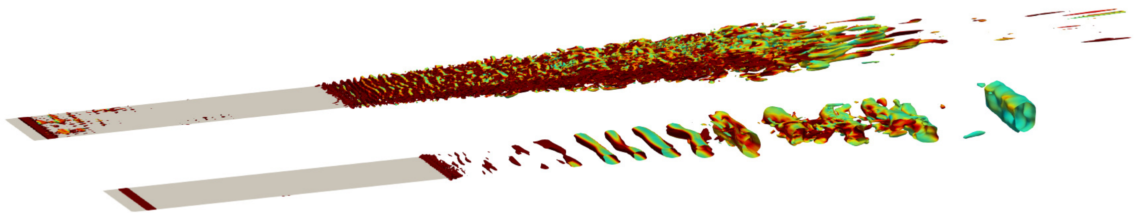

Figure 6. Q-criterion isosurfaces coloured with vorticity magnitude, computed by EARSM-DDES (top) and $k-\omega$ SST-DDES (bottom).

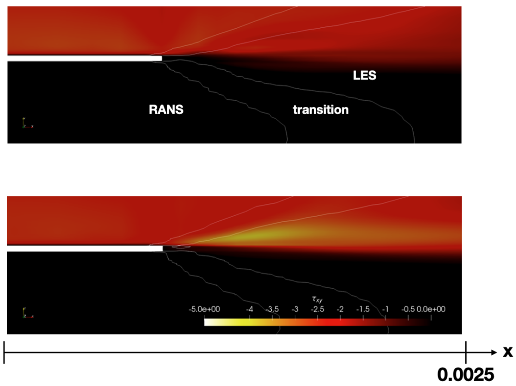

Figure 7. Mixing layer simulation using EARSM-DDES (top) and SST-DDES (bottom) showing SGS shear stress τ_{xy} and iso-lines of the blending function $f_d = 0.1$ and 0.9.

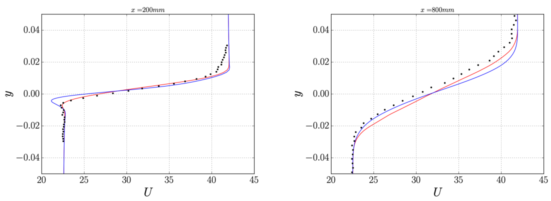

Figure 8. Mixing layer simulation using DDES. Computed velocity profiles at $x = 200$ (left) and 800 (right) using SST-DDES (blue) and EARSM-DDES (red) compared with experiments (symbols).

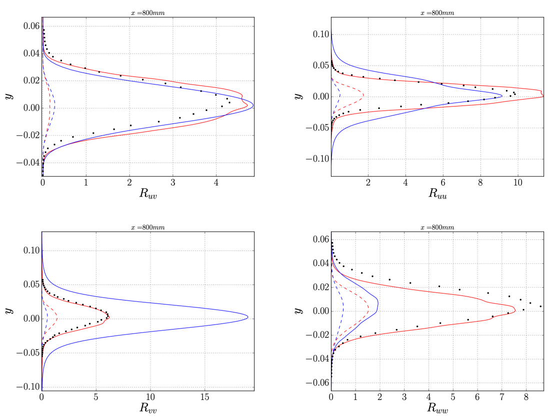

Figure 9. Mixing layer simulation using DDES. Computed Reynolds stress profiles at $x = 800$ using SST-DDES (blue) and EARSM-DDES (red) compared with experiments (symbols). Dashed curves shows the modelled, or SGS, part of the stress.

SST-(I)DDES. However, the blending function is non linear and might be influenced through the coupling with the accompanying k-ω model equations where the production term is differently modelled. The other explanation is that the EARSM might introduce a more physically correct modelling with, in particular, a different response to non-equilibrium conditions typically for these transition regions.

Some recent studies on mitigating the grey-area problem are focused on directly reducing the length-scale definition by measuring the amount of resolved turbulence, e.g. the sigma model, see e.g. Fuchs *et al.* (2020). Moreover, the commutation term emerging from the rapid change of resolution, here measured by the transition from RANS to LES length scales, might be of large importance. Further studies in this direction should include the tentative modelling of this phenomenon proposed by Girimaji & Wallin (2013). These phenomena are basically independent and should be combined for a more general and consistent approach.

This work has been funded by the Swedish Governmental Agency for Innovation Systems (VINNOVA) in the Swedish National Flight Research Program (NFFP-CIAO, Contract No. 2017-04887). Computer time has been provided by the Swedish National Infrastructure for Computing (SNIC).

REFERENCES

Cherry, Erica M, Elkins, Christopher J & Eaton, John K 2008 Geometric sensitivity of three-dimensional separated flows. *International Journal of Heat and Fluid Flow* **29** (3), 803–811.

Fuchs, Marian, Mockett, Charles, Sesterhenn, Jörn & Thiele, Frank 2020 The grey-area improved σ-ddes approach: Formulation review and application to complex test cases. In *Progress in Hybrid RANS-LES Modelling*, pp. 119–130. Springer.

Germano, Massimo, Piomelli, Ugo, Moin, Parviz & Cabot, William H 1991 A dynamic subgrid-scale eddy viscosity model. *Physics of Fluids A: Fluid Dynamics* **3** (7), 1760–1765.

Girimaji, Sharath S & Wallin, Stefan 2013 Closure modeling in bridging regions of variable-resolution (vr) turbulence computations. *Journal of Turbulence* **14** (1), 72–98.

Gritskevich, Mikhail S, Garbaruk, Andrey V, Schütze, Jochen & Menter, Florian R 2012 Development of DDES and IDDES formulations for the k-ω shear stress transport model. *Flow, turbulence and combustion* **88** (3), 431–449.

Jaffrézic, B & Breuer, M 2008 Application of an explicit algebraic Reynolds stress model within a hybrid LES–RANS method. *Flow Turbul. Combust.* **81** (3), 415.

Kamble, Chetna, Girimaji, Sharath, Razi, Pooyan, Tazraei, Pedram & Wallin, Stefan 2022 Closure modeling in near-wall region of steep resolution variation for partially averaged navier-stokes simulations. *Phys. Rev. Fluids* **7**, 044608.

Marstorp, Linus, Brethouwer, Geert, Grundestam, Olof & Johansson, Arne V 2009 Explicit algebraic subgrid stress models with application to rotating channel flow. *Journal of Fluid Mechanics* **639**, 403–432.

Mellen, CP, Fröhlich, J & Rodi, W 2000 Large eddy simulation of the flow over periodic hills. In *16th IMACS world congress*, pp. 21–25.

Mockett, C, Haase, Werner & Schwamborn, Dieter 2018 *Go4Hybrid: Grey Area Mitigation for Hybrid RANS-LES Methods*, , vol. 134. Springer.

Montecchia, Matteo 2019 Numerical and modelling aspects of large-eddy and hybrid simulations of turbulent flows. PhD thesis, KTH Royal Institute of Technology.

Montecchia, Matteo, Brethouwer, Geert, Johansson, Arne V & Wallin, Stefan 2017 Taking large-eddy simulation of wall-bounded flows to higher reynolds numbers by use of anisotropy-resolving subgrid models. *Physical Review Fluids* **2** (3), 034601.

Montecchia, Matteo, Brethouwer, Geert, Wallin, Stefan, Johansson, Arne V & Knacke, Thilo 2019 Improving LES with OpenFOAM by minimising numerical dissipation and use of explicit algebraic SGS stress model. *Journal of Turbulence* pp. 1–26.

Montecchia, Matteo, Knacke, Thilo, Brethouwer, Geert, Wallin, Stefan & Johansson, Arne V. 2018 Improved LES of turbulent channel flow by using OpenFOAM with the Explicit Algebraic SGS model. *12th International ERCOFTAC Symposium on Engineering Turbulence Modelling and Measurements* .

Ohlsson, Johan, Schlatter, Philipp, Fischer, Paul F & Henningson, Dan S 2010 Direct numerical simulation of separated flow in a three-dimensional diffuser. *Journal of Fluid Mechanics* **650**, 307–318.

Spalart, Philippe R 2009 Detached-eddy simulation. *Annual review of fluid mechanics* **41**, 181–202.

Wallin, Stefan & Johansson, Arne V 2000 An explicit algebraic Reynolds stress model for incompressible and compressible turbulent flows. *Journal of Fluid Mechanics* **403**, 89–132.